Particularities of overdetermined linear systems arising in particle size analysis

D. Calistru, R. Mondescu, I. Baltog

Classification
Physics Abstracts
42.20G — 02.60

Particularities of overdetermined linear systems arising in particle size analysis

D. M. Calistru, R. Mondescu and I. Baltog

Institute of Atomic Physics, I.F.T.A.R., Lab. 22, P.O. Box MG-6, R-76900 Magurele-Bucharest, Romania

(Received 25 July 1991, revised 25 February 1992, accepted 1 April 1992)

Abstract. — This paper presents a specific data processing algorithm for particle size analysis and a subsequent study under regarding its performances and limitations accidental input data errors and the limit of resolution of the algorithm.

Introduction.

The precision of particle size distribution analysis by light scattering depends on two main features : the measurement precision in the observation plane of the light scattered by a given particle distribution, and the computation algorithm and its susceptibility to accidental input data error. The physical phenomenon is described by the theory of Fraunhofer diffraction on a circular aperture. This paper presents a method for data processing in light scattering experiments and their response to accidental errors.

1. Theoretical background of particle size analysis.

1.1 PHYSICAL ASPECTS. — The intensity of the light scattered by a spherical particle of diameter a measured along an axis which makes an angle θ with the incident direction is

$$i(a, \theta) = C \left(\frac{\pi a^2}{4} \right)^2 \left[\frac{2 J_1 \left(\frac{\pi a}{\lambda_0} \sin \theta \right)}{\frac{\pi a}{\lambda_0} \sin \theta} \right]^2 \tag{1}$$

where λ_0 is the wavelength of the incident monochromatic light', $J_1(x)$ is a Bessel function of order 1, and C is a constant ($C > 0$). The energy diffracted by the spherical particle in the ring of radii r_{int} and r_{ext} in the observation plane is given by :

$$e(a, r_{int}, r_{ext}) = C a^2 [J_0^2(x_{int}) + J_1^2(x_{int}) - J_0^2(x_{ext}) - J_1^2(x_{ext})] \tag{2}$$

with

$$x_{\text{int, ext}} = \frac{\pi a}{\lambda_0} \sin\left(\text{arctg}\left(\frac{r_{\text{int, ext}}}{f}\right)\right) \tag{3}$$

f being the focal length of the lens (the detecting cell is placed in the focal plane) and $J_0(x)$ is the Bessel function of order 0.

Considering a volumetric particle size distribution $v(a)$, (2) becomes

$$e(r_{\text{int}}, r_{\text{ext}}) = C_1 \int_{d_{\min}}^{d_{\max}} \mathfrak{L}(a, r_{\text{int}}, r_{\text{ext}}) \frac{v(a)}{a} \, da \tag{4}$$

with

$$\mathfrak{L}(a, r_{\text{int}}, r_{\text{ext}}) = J_0^2(x_{\text{int}}) + J_1^2(x_{\text{int}}) - J_0^2(x_{\text{ext}}) - J_1^2(x_{\text{ext}}) \tag{5}$$

and $d_{\max}$, $d_{\min}$ the maximum and minimum diameters respectively of the considered distribution, $\{e_j(r_{\text{int}}, r_{\text{ext}})\}$ $j = \overline{1, m}$ stand for the real measured values which permit the determination of $v(a)$, and m is the number of detecting cells.

The data processing raises two theoretical problems :

1) The influence of measurement errors on the values $\{e_j(r_{\text{int}}, r_{\text{ext}})\}$.

2) Solving an ill — conditioned linear system with m equations. Both aspects will be further analysed and discussed.

1.2 MATHEMATICAL ASPECTS. — From the mathematical point of view (4) is a first rank Fredholm equation

$$e(r_{\text{int}}, r_{\text{ext}}) = \int_{d_{\min}}^{d_{\max}} K(a, r_{\text{int}}, r_{\text{ext}}) \, v(a) \, da \tag{6}$$

$$K(a, r_{\text{int}}, r_{\text{ext}}) = C_1 \frac{\mathfrak{L}(a, r_{\text{int}}, r_{\text{ext}})}{a} \tag{6a}$$

$K(a, r_{\text{int}}, r_{\text{ext}})$ is the kernel of the integral equation, $v(a)$ the unknown volumetric distribution (which will be determined) and $e(r_{\text{int}}, r_{\text{ext}})$ discrete experimentally measured data. Considering the detection system as being formed of m detecting cells, $e(r_{\text{int}}, r_{\text{ext}})$ is a vector in the following notation

$$e = \{e_j\}_{j = \overline{1, m}} = \{e_j(r_{\text{int}_j}, r_{\text{ext}_j})\}_{j = \overline{1, m}} . \tag{7}$$

The distribution $v(a)$ is approximated within its definition range $\{d_{\min}, d_{\max}\}$ with a sum of n Gauss-type functions. The assumption of non-gaussian type functions used in the solving of this particular problem will be discussed further. The analytical form for the Gauss-type functions which appear in the expansion of $v(a)$ is the log-normal one and is given in (9). This is one of the most frequent forms used in particle size distribution problems [2]. We will approximate

$$v(a) = \sum_{k=1}^{n} c_k \, g_k(a) \tag{8}$$

with

$$g_k(a) = e^{-\frac{(\ln a - \ln \bar{a}_k)}{2}} ; \qquad k = \overline{1, n} \tag{9}$$

c_k is the weight contribution of $g_k(a)$ in the approximation of the volumetric distribution, $\bar{a}_k$ — the median value for the log-normal distribution $g_k(a)$, and σ is the distribution's dispersion. Equation (6) becomes :

$$e_j(r_{\text{int}_j}, r_{\text{ext}_j}) = \int_{d_{\min}}^{d_{\max}} K(a, r_{\text{int}}, r_{\text{ext}}) \sum_{k=1}^{n} c_k\, g_k(a)\, \mathrm{d}a$$

$$= \sum_{k=1}^{n} c_k \left(\int_{d_{\min}}^{d_{\max}} K(a, r_{\text{int}}, r_{\text{ext}})\, g_k(a)\, \mathrm{d}a \right)$$

$$= \sum_{k=1}^{n} c_k K_{kj}, \quad j = \overline{1, m} \tag{10}$$

(10) is a linear system with m equations and n unknowns. We can write it in the vectorial form as

$$e = Kc \tag{11}$$

where

$$e = \left\{ e_j(r_{\text{int}_j}, r_{\text{ext}_j}) \right\}_{j = \overline{1, m}} \tag{11a}$$

$$c = \{c_k\}_{k = \overline{1, n}} \tag{11b}$$

$$K = \{K_{kj}\}_{\substack{k = \overline{1, n} \\ j = \overline{1, m}}} . \tag{11c}$$

The problem is reduced to determining the weights $\{c_k\}$ which permits according to (8) the approximation of the volumic distribution $v(a)$. The inequality $m \geq n$ is obvious, the system being otherwise undetermined. We are constrained to consider at the most $n = m$ unknowns (granulometric classes). In this case we have to solve a linear ill-conditioned system. Thus we have to apply a regularisation method [3, 4] each with its own advantages and disadvantages. We have experimented the Tikhonov regularisation method which minimizes the functional

$$M^{\alpha}_{[c]} = \sum_{j=1}^{m} \left(\sum_{k=1}^{m} K_{jk}\, c_k - e_j \right)^2 + \alpha \sum_{k=1}^{m} c_k^2 \tag{12}$$

α being the regularisation parameter. Applying this method on two different solving methods for (11), namely using eigenvalues and a functional we found maxima shiftings and the existence of local quasiperiodical parasitic maxima. Furthermore, the algorithm revealed an exaggerated sensitivity to accidental input data fluctuations (less than 5 %).

These results led us to an alternative for solving (11), namely treating it as an overdetermined system ($m \geq n$). The normal equations were obtained by the least-squares solution method of an overdetermined system, which in turn, was solved by Gauss elimination [5].

After solving (11), the solution vector $\{c_k\}_{k = \overline{1, n}}$ will be obtained. Let us assume the real case for determining the distribution $v(a)$, where only some granulometric classes have an effective contribution, the rest having null contribution. Thus, in the real case $\{c_k \geq 0\}_{k = \overline{1, n}}$ Any $\{c_i\} < 0$ have no physical meaning. Because the solutions are not exactly determined, their computed values will show deviations, both positive and negative, from the real values. Hence, we expect the presence of negative computed weights $\{c_i\} < 0$. We suggest overcoming this impediment as follows. We search for the minimum c value, which will be denoted as $\{c_{\min}\}$. If $c_{\min} \geq 0$, the solutions have physical meaning and we can determine

$v(a)$ from (8). If $c_{\min} < 0$ we impose $c_{\min} = 0$ based on the following motivation. The minimum (negative) computed value ($\{c_{\min}\}$) is necessarily « associated with » the real minimum value (null) because the hierarchy of the coefficients is not altered by their computation i.e. by solving (11). This process, which will be an iterative one, alters only the values of the coefficients. Noting that $\{c_{\min}\} = 0$ multiplies the components $\{K_{j,\min}\}$ this equates to their annulment. We are now at the point of solving an over-determined system with m equations and $n - 1$ unknowns. This process will be iterated until all the solutions are null or positive $\{c_k \geqslant 0\}_{\substack{k = \overline{1,p} \\ p < n}}$. Being careful to store the ranks of the imposed null coefficients we will reconstruct c thus obtaining the weights which rebuild the volumic distribution $v(a)$.

A very important problem is that of choosing the mean diameters for each class $\{\bar{a}_k\}_{k = \overline{1,n}}$ and σ (for (9)).

Previous studies [6] have shown that instability attenuation is improved by choosing a geometrically increasing length for the granulometric classes. The ratio of the geometrical progression is

$$R = \left(\frac{d_{\max}}{d_{\min}} \right)^{1/n} \tag{13}$$

The mean diameter $\bar{a}_k$ was chosen as the mid length interval for the k-th class in a logarithmic scale :

$$\ln \bar{a}_k = \frac{\ln (d_{\min} \cdot R^{k-1}) + \ln (d_{\min} \cdot R^{k})}{2} \tag{14}$$

The σ value determines the « coverage » of the log-normal distributions. High σ values imply a greater degree of superposition, leading to a lower scale sensitivity. Low σ values imply a smaller degree of superposition and a consequent greater fluctuation in $\{c_k\}$ values. The minimum value can be determined by imposing a single maximum for the function obtained as the sum of two consecutive $g_k(a)$ functions

$$\begin{cases} f(x) = e^{-\frac{(x - \ln \bar{a}_k)^2}{2}} + e^{-\frac{(x - \ln \bar{a}_{k+1})^2}{2}} ; \quad x = \ln a \\ f'(x) = 0 \\ f''(x) = 0 . \end{cases} \tag{15}$$

This leads to

$$\sigma \geqslant \frac{1}{2} \ln R . \tag{16}$$

The maximum σ value is that where $g_k(a) = 1/2$ on the maxima of the neighbouring log-normal functions (g_{k-1}, g_{k+1})

$$\sigma = \frac{1}{\sqrt{2 \ln 2}} \ln R \tag{17}$$

$$\sigma \in \left[\frac{\ln R}{2}, \frac{\ln R}{\sqrt{2 \ln 2}} \right] . \tag{18}$$

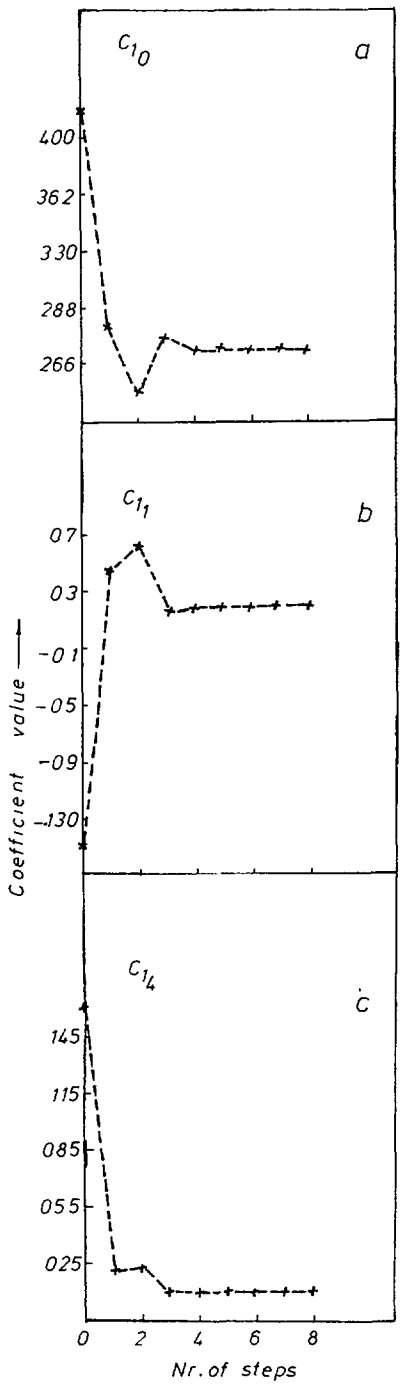

Fig. 1. — The evolution of three particular solutions (c_{10}, c_{11}, c_{14}) during the iterative solving process for a simulated distribution given by (9), with $\bar{a} = 68.3$ μm and $\sigma = 0.2372$ (a) $- c_{10}$ b) $- c_{11}$, c) $- c_{14}$).

We chose

$$\sigma = \frac{3 \ln R}{4\sqrt{2 \ln 2}} \simeq 0.64 \ln R \,. \tag{18a}$$

Further chosen (or imposed data) were : $m = 16$ (the detecting system is formed of 16 cells), $d_{min} = 2$ μm, $d_{max} = 360$ μm, $\lambda_0 = 0.6328$ μm, $f = 200$ mm and $n = 14$.

2. Results and discussion.

Working in the previously mentioned conditions we developed a routine which tested the following simulated situations :

A. Recurrent solution evaluation for equation (11).
B. Monomodal curve analysis with no input data errors.
C. Monomodal curve analysis with ± 10 % and ± 20 % input data errors.
D. Bimodal curve analysis, having the same amplitude.
E. Bimodal curve analysis, of different amplitudes, with ± 10 % and ± 20 % input data errors.

2.1 RECURRENT SOLUTION EVALUATION FOR EQUATION (11). — Studying the evolution of the n solutions of (11) when recurrently imposing $\{c_{min}\} = 0$, we observed their convergence towards stable values. Figure 1 shows the evolution of three particular solutions ($\{c_{10}\}$, $\{c_{11}\}$, $\{c_{14}\}$) during the iterative solving process for a simulated distribution given by (9), with $\bar{a} = 68.3$ μm and $\sigma = 0.2372$. The three particular solutions become stable after four iterations. Nevertheless the recurrent solving is carried on until all $\{c_k \geq 0\}_{k = \overline{1,16}}$ which is a stronger requirement than the stability conditions.

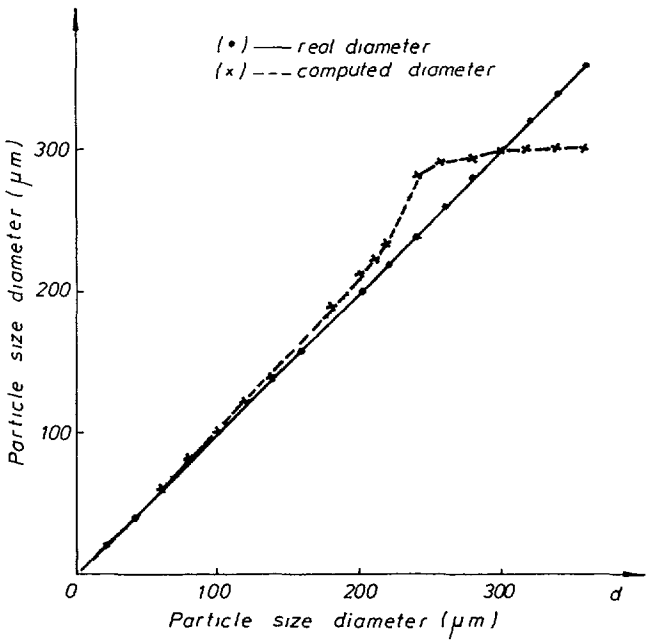

Fig. 2. — Simulated and computed maxima values for monomodal curves with no input data errors.

2.2 MONOMODAL CURVE ANALYSIS WITH NO INPUT DATA ERRORS. — We studied the range $a \in [2.5, 360]$ μm. The relative deviations of maxima for the simulated and computed values are < 5 % for $a \in (2.5, 160)$ μm and < 10 % for $a \in (160, 220)$ μm. The routine does not discern further variations of maxima in the range (300, 360) μm, displaying a constant value : $a = 300$ μm. Figure 2 shows the decrease in precision for several monomode curves. This study offers the opportunity to adopt an appropriate correction for the final solution in order to permit an accurate evaluation of maxima in the range (160, 220) μm.

2.3 MONOMODAL CURVE ANALYSIS WITH ± 10 % AND ± 20 % INPUT DATA ERRORS. — Since the input data in the real measuring process may be altered and error affected, this phenomenon was simulated in the numerical input data with maximum ± 10 % and maximum ± 20 % input data alteration, respectively. We noticed a greater susceptibility to a error

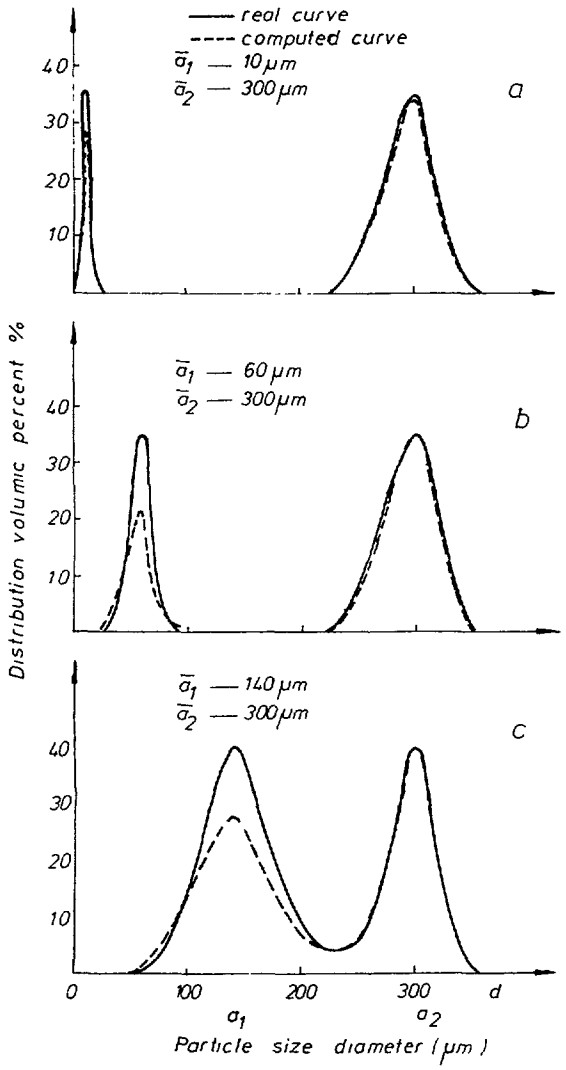

Fig. 3. — Bimodal curves having the maxima at : a) $\bar{a}_1 = 10$ μm, b) $\bar{a}_1 = 60$ μm, c) $\bar{a}_1 = 140$ μm and $\bar{a}_2 = 300$ μm in all three cases. Simulated (———) and computed (·····) profile comparison.

affected data in the low particle range. Thus, at maximum ± 20 % input data errors, with distributions centred at low values ($a < 30$ μm), parasitic maxima may arise and a consequent modification of the class distribution. Yet for maximum ± 10 % input data errors, both the maxima positioning and particle size class distribution are preserved on the whole range. Special care should be devoted to detection precision in the low particle range, which means an appropriate sensitivity in the peripheral collecting areas.

2.4 BIMODAL CURVE ANALYSIS HAVING THE SAME AMPLITUDE. — A case often met in practice is that of bimodal distributions. We have analysed such a simulated distribution by fixing the maximum of one curve ($a_2 = 300$ μm — the limiting sensitivity value discussed in 2.2), and shifting the maximum (a_1) of the second curve over the range up to 160 μm. We studied the range [2.5, 360] μm. The routine discerns the separated curves only for $\bar{a}_1 \leqslant 160$ μm. This should not be a surprising fact. Two maxima can be separated only if a local minimum exists between them. Due to the geometric increase in class width, $a > 160$ μm and $a = 300$ μm are situated in two consecutive classes and the superposition of their corresponding distributions no longer generates a local minimum.

Figure 3 shows the deviation of computed curves from simulated ones for three curve pairs having their corresponding maxima at : a) $a_1 = 10$ μm ; b) $a_1 = 60$ μm ; c) $a_1 = 140$ μm and $a_2 = 300$ μm in all cases. When altering the input data by at most ± 10 % and ± 20 % respectively a good maxima stability and procentual class distribution is revealed, mainly for ± 10 %.

2.5 BIMODAL CURVE ANALYSIS, OF DIFFERENT AMPLITUDES, WITH ± 10 % AND ± 20 % INPUT DATA ERRORS. — We considered the superposition of two monodisperse distributions (C_1 and C_2) having different weights, namely : ($a_1 = 89$ %, $a_2 = 11$ %), ($b_1 = 83$ %, $b_2 = 17$ %), ($d_1 = 77$ %, $d_2 = 23$ %) in the following cases :

a) $a_1 C_1 + a_2 C_2$
b) $a_2 C_1 + a_1 C_2$
c) $b_1 C_1 + b_2 C_2$
d) $b_2 C_1 + b_1 C_2$
e) $d_1 C_1 + d_2 C_2$
f) $d_2 C_1 + d_1 C_2$.

Each case was submitted to a maximum input data alterations of ± 10 % and ± 20 % respectively. We worked with the following pairs :

I) $C_1 . \bar{a}_1 = 16.8$ μm, $C_2 . \bar{a}_2 = 290$ μm
II) $C_1 . \bar{a}_1 = 27.8$ μm, $C_2 . \bar{a}_2 = 68.3$ μm
III) $C_1 . \bar{a}_1 = 102$ μm, $C_2 . \bar{a}_2 = 290$ μm .

The simulation showed that for a single curve contribution less than 11 % in a bimodal distribution a) and b) the routine does not discern the two different maxima. Otherwise c)-f) they are well separated and positioned, even at ± 10 % input data errors. The input errors of maximum ± 20 % modify only the hystogram's profile, not the maxima positions, within the limits discussed at 2.2.

The most important conclusion is the lack of effectiveness in the system's capability of data collecting and processing for mass contributions < 10 % in a given bidisperse distribution. The situation is relaxed in polymodal distributions.

Conclusions.

The routine succeeds in correctly positioning simulated mono- and bimodal (with different weights) curve maxima even at input data errors of ± 10 %. Consequently, the experimental determinations should be conducted with care in order not to exceed the security limit. At input errors of ± 20 %, although the maxima position is still reliable, we may observe a more dramatic percentage modification in class distribution, especially in the lower range ($a < 30$ μm).

The routine reveals monomodal curve contributions beginning at 10-15 % in a more complex profile.

Presently, the routine is being upgraded and extended with an initial input data processing (smoothing) routine in order to minimize the influence of accidental errors. Another alternative routine will be aimed at solving (11) by using in (8) other distribution profiles (e.g. Rosin-Rammler) instead of the log-normal one and/or a different degree of coverage (another σ), with distinctions among classes.

References

[1] CORNILLAULT J., Particle Size Analyser, *Appl. Opt.* **11** (Febr. 1972) 265-268.
[2] MERCER T. T., Aerosol Technology in Hazard Evaluation (Academy Press, 1973).
[3] PROVENCHER S. W., A Constrained Regularization Method for Inverting Data Represented by Linear Algebraic or Integral Equations, *Comput. Phys. Commun.* **27** (1982) 213-227.
[4] KAZOWSKI L. B., Particle Analysis Using Forward Scattering Data, *Appl. Opt.* **23** (1984) 448-454.
[5] SCHEID F., Numerical Analysis, Schaum's Outline Series (McGraw-Hill Book Company, 1968).
[6] CORNILLAULT J. *et al.*, High Resolution Submicronic Granulometer, *Electr. Commun.* **61** (1987) 446-452.